Microtubules in the fungal pathogen *Ustilago maydis* are highly dynamic and determine cell polarity

Gero Steinberg*, Roland Wedlich-Söldner, Marianne Brill‡ and Irene Schulz

Institut für Genetik und Mikrobiologie, LMU, Maria-Ward-Straße 1a, D-80638 München, Germany

‡Present address: Institut für med. Mikrobiologie, Immunologie und Hygiene, LMU, Trogerstraße 4a, D-81675 München, Germany

*Author for correspondence at present address: Max Planck Institut für Terrestrische Mikrobiologie, Karl von Frisch Straße, D-35043 Marburg, Germany (e-mail: Gero.Steinberg@mailer.uni-marburg.de)

Accepted 18 November 2000

Journal of Cell Science 114, 609-622 © The Company of Biologists Ltd

SUMMARY

Many fungal pathogens undergo a yeast-hyphal transition during their pathogenic development that requires rearrangement of the cytoskeleton, followed by directed membrane traffic towards the growth region. The role of microtubules and their dynamic behavior during this process is not well understood. Here we set out to elucidate the organization, cellular role and in vivo dynamics of microtubules in the dimorphic phytopathogen *Ustilago maydis*. Hyphae and unbudded yeast-like cells of *U. maydis* contain bundles of spindle pole body-independent microtubules. At the onset of bud formation two spherical tubulin structures focus microtubules towards the growth region, suggesting that they support polar growth in G_2, while spindle pole body-nucleated astral microtubules participate in nuclear migration in M and early G_1. Conditional mutants of an essential α-tubulin gene from *U. maydis*, *tub1*, confirmed a role for interphase microtubules in determination of cell polarity and growth. Observation of GFP-Tub1 fusion protein revealed that spindle pole body-independent and astral microtubules are dynamic, with elongation and shrinkage rates comparable to those found in vertebrate systems. In addition, very fast depolymerization was measured within microtubule bundles. Unexpectedly, interphase microtubules underwent bending and rapid translocations within the cell, suggesting that unknown motor activities participate in microtubule organization in *U. maydis*.

Movies available on-line:
http://www.biologists.com/JCS/movies/jcs1792.html

Key words: Pathogenic fungus, Polar growth, Green fluorescent protein, Microtubule, Motility

INTRODUCTION

Many eukaryotic cells are able to follow external stimuli by rearrangement of their cytoskeleton and subsequent membrane traffic towards polarized cellular domains. Filamentous actin and microtubules (MTs) in combination with associated proteins, like molecular motors, support this process by directed delivery of growth supplies during polar growth of some plant cells (Bibikova et al., 1999), vertebrate cells (Nabi, 1999) and fungi (Heath, 1995; Mata and Nurse, 1998). In contrast to actin fibres, MTs support long distance transport processes and thereby determine directionality of cell extension (Nabi, 1999). MTs consist of globular tubulin subunits that slowly polymerize and rapidly depolymerize at their plus-ends (Desai and Mitchison, 1997). This dynamic behavior, in combination with translocation of complete MTs (see Tanaka and Kirschner, 1991; Vorobjev et al., 1997), enables vertebrate cells to react to external stimuli and allows adaptation to specialized functions (reviewed by Joshi, 1998). In fungi, dynamics of green fluorescent protein (GFP)-tubulin-containing MTs were described for *Saccharomyces cerevisiae* (Carminati and Stearns, 1997; Shaw et al., 1997; Maddox et al., 1999; Maddox et al., 2000; Adames and Cooper, 2000) and *Schizosaccharomyces pombe* (Ding et al., 1998; Mallavarapu et al., 1999; Yamamoto et al., 1999; Drummond and Cross, 2000), and these studies revealed an involvement of MTs in nuclear migration and mitosis.

Many fungi are able to switch between yeast-like and hyphal growth, thereby adapting to special requirements during their life cycle (Carlile, 1995). In particular, yeast-hyphal dimorphism is a common feature of many human and plant pathogens including *Candida albicans*, *Histoplasma capsulatum* and *Ustilago maydis* (reviewed in Gow, 1995). Dimorphic transitions require the perception of external stimuli that induce the reorganization of the cytoskeleton followed by polar delivery of vesicles containing biosynthetic enzymes, membrane components and wall ingredients towards the expanding growth region. Therefore, it is thought that cytoskeleton-based membrane transport plays a key role in pathogenic development of these fungi (Gow, 1995).

The dimorphic fungus *Ustilago maydis* is the causative agent of corn smut disease and causes considerable losses of grain yield (Agrios, 1999). Outside the plant the fungus exists as haploid yeast-like cells that grow by budding at the poles of the elongated cell (Jacobs et al., 1994). On the plant epidermis two cells of opposite mating types can fuse and give rise to a filamentous dikaryotic hypha, which advances over the plant surface and penetrates the host tissue. Inside the plant the fungus proliferates and tumor formation is induced, followed by karyogamy and sporogenesis (reviewed in Banuett, 1995).

Under laboratory conditions *U. maydis* can be easily cultured and is accessible to both genetic and molecular methods. Therefore, this fungal pathogen is well suited for the investigation of the molecular basis of pathogenicity and dimorphism (reviewed in Banuett, 1995). However, an understanding of the cellular organization of this pathogen and the role of the cytoskeleton in growth, dimorphism and pathogenicity is only at its beginning. These initial studies have revealed that microtubule-dependent organelle transport plays a key role in polar growth (Wedlich-Söldner et al., 2000) and hyphal elongation (Lehmler et al., 1997).

In this study we have investigated the organization and dynamic behaviour of MTs in *U. maydis*. Immunofluorescence studies and mutant analysis indicate a role of MTs in polar budding, morphogenesis and nuclear migration. In vivo analysis of GFP-Tub1 fusion protein demonstrate that MTs are dynamic during interphase and mitosis. Moreover, similar to vertebrate cells, MTs show bending and motility within the cell.

MATERIALS AND METHODS

Strains and growth conditions

U. maydis strains FB1 (*a1b1*) and FB2 (*a2b2*) have been described previously (Banuett and Herskowitz, 1989). Strain SG200 (*a1 mfa2 bW2 bE*) is a derivative of SG100 (Bölker et al., 1995a) that grows filamentous on charcoal-containing solid medium and was used to investigate the hyphal stages of *U. maydis*. FB2rGFPTub1 and SG200rGFPTub1 were generated by integration of plasmid prGFPTub1 into the succinate-dehydrogenase locus of strain FB2 and SG200, respectively. FB1otefGFPTub1 and FB2otefGFPTub1 contained plasmid potefGFPTub1 integrated into the succinate-dehydrogenase locus of wild-type strain FB1. In strain FB2rTub1 the *tub1* gene is under the control of the *crg*-promoter (Bottin et al., 1996) and integrated by homologous recombination into the *tub1* locus of FB2. All transformation was done as described (Schulz et al., 1990). If not otherwise mentioned strains were grown at 28°C in 2.5% potato dextrose (PD) or complete medium (CM; Holliday, 1974) supplemented with 1% glucose (CM-G) or 1% arabinose (CM-A), respectively. Solid media contained 2% (w/v) bacto-agar. To generate dikaryotic hyphae for immunofluorescence, compatible strains were cospotted on charcoal-containing agar plates and incubated at room temperature. To investigate FB2rTub1 mutants, cells were grown overnight in CM-A washed with 1 volume CM-G diluted 1:10 in 10 ml CM-G and incubated in a shaker at 28°C, 200 r.p.m.

Identification of tub1

The *tub1* gene was isolated via PCR using degenerate primers and genomic DNA of *U. maydis*. Primers were directed against conserved regions that are specific for α-tubulins. PCR was done using 30 cycles of 95°C, 1 minute; 52°C, 1 minute; 72°C, 2 minutes and primers TubA2 (AAYCARATGGTNAARTGYGAYCC) in combination with the reverse primers TubA3 (TTRAADCCIGTNGGRCACCARTC) or TubA4 (ACRTACCARTGIACRAANGCDCG). DNA fragments of 156 bp and 342 bp were sequenced and used to identify a full-length clone in a cosmid library (Bölker et al., 1995b). All subsequent cloning was done using *Escherichia coli* K12 strain DH5α (Bethesda Research Laboratories) following standard protocols (Sambrook et al., 1989).

Plasmid constructions

pTub1E

A 3.5 kb *Eco*RI fragment, which contained the full-length *tub1* gene, was cut out of a cosmid and cloned into pUC18 to give pTub1E.

prGFPTub1

The N-terminal eGFP-Tub1 fusion under the control of the *crg*-promoter was generated in three steps. The open reading frame of *tub1* was amplified from pTub1E generating an *Nde*I site at the start codon and an *Eco*RI site 383 bp downstream of the 3′ end of *tub1* (Pfu-polymerase, primers: TubA15 (CGGAATTCACATTTCGCAATCC-GAT), TubA16 (GCCATATGCGTGAAGTTCTTTCC)). This fragment was cloned into pCR®2.1-TOPO (Invitrogen) and sequenced. eGFP (Clontech) was excised from p630 (A. Hartmann, unpublished) as a *Nco*I-*Nde*I fragment. The *crg*-promoter was obtained as a *Kpn*I-*Nco*I fragment of 3.6 kb from p194 (A. Brachmann and R. Kahmann, unpublished). In a four-fragment ligation these DNA fragments were cloned into the *Kpn*I-*Eco*RI digested backbone from p123 (C. Aichinger, unpublished) that contained the carboxin resistance cassette. After digestion with *Ssp*I the construct was integrated by homologous recombination into the succinate-dehydrogenase locus.

potefGFPTub1

To put the eGFP-*tub1* fusion construct under the control of the constitutive *otef*-promoter (Spellig et al., 1996) an *Sbf*I-*Nco*I fragment from p123 containing the *otef*-promotor was used to replace the *crg*-promotor in prGFPTub1 (ligated to an *Nco*I-*Eco*NI fragment and an *Eco*NI-*Sbf*I fragment from prGFPTub1).

pcrgTub1

This plasmid was used for the integration of the *crg*-promoter in front of the *tub1* gene to create conditional mutants of *tub1*. The construction was done in two steps. The 5′ flanking region, containing 556 bp from the *tub1*-promoter up to the ATG, was amplified by PCR from pTub1E, thereby generating two restriction sites (*Eco*RI-*Kpn*I). This fragment, together with a 3.6 kb *crg*-promoter fragment (*Kpn*I-*Nde*I) from prGFPTub2 (G. Steinberg and M. Brill, unpublished) and a 1506 bp 3′ flank (*Nde*I-*Nco*I) containing the 5′ region of *tub1* from prGFPTub1, was ligated into pSL1180 digested with *Mun*I and *Nco*I. In a second step a *Bam*HI-*Pml*I fragment from pSLHyg(+) (A. Brachmann, unpublished) containing a hygromycin resistance cassette was inserted in front of the *crg*-promoter into *Bam*HI-*Sma*I.

Western analysis

For preparation of protein extracts logarithmic cultures were harvested by centrifugation at 3000 r.p.m. Cell pellets were washed in cold AP100 (100 mM Pipes, 2 mM $MgCl_2$, 1 mM EGTA, 1 mM EDTA, protease inhibitor; Boehringer, Ingelheim) and disrupted in a French Press at 1,100 psi. Protein concentration was measured according to Bradford, 1976, and equal amounts of protein were loaded and separated by SDS-PAGE. Subsequent western blots were essentially done as described (Steinberg and Schliwa, 1995).

Light microscopy and image processing

Cells from logarithmically grown cultures were embedded in 1% pre-warmed low-melt agarose and immediately observed using a Zeiss Axiophot microscope. For motion analysis 60-frame sequences of single cells were taken at 500 millisecond intervals using a cooled CCD camera (Hamamatsu, C4742-95). Epifluorescence was observed using standard FITC, DAPI and Rhodamine filter sets. For colocalization studies eGFP fluorescence was detected by a specific filter set (BP 470/20, FT 493, BP 505-530, Zeiss). Image processing and measurements were done with Image-Pro Plus (Media Cybernetics) and Photoshop (Adobe). Statistical analyses using unpaired *t*-tests or Mann-Whitney test that do not assume a Gaussian distribution were performed using PRISM (GraphPad).

Quantitative analysis of MT dynamics

For quantification of the parameters of MT dynamics, sequences of 60 images at intervals of 500 milliseconds were taken. From these sequences growth and shrinkage rates, catastrophe and rescue values

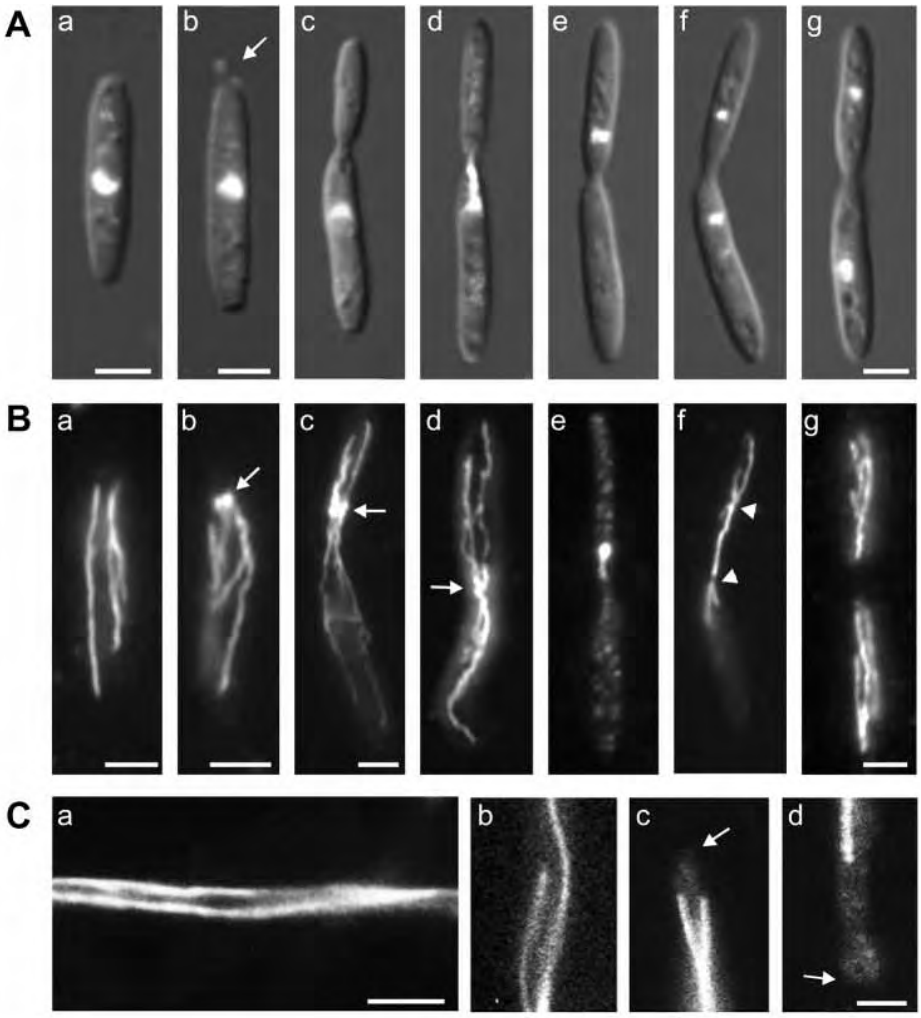

Fig. 1. Nuclear movement and microtubule organization in *U. maydis*. (A) Overlay of epifluorescence of nuclear DAPI-staining and light microscopy of haploid *U. maydis* cells. During most stages of budding the nucleus remains positioned in the middle of the mother cell (a-c). Prior to mitosis, the nucleus migrates into the bud (d) and mitosis occurs (e). This is followed by the separation of the condensed daughter nuclei (f) and subsequent positioning in mother and daughter cell, respectively (g). Bars, 3 μm. (B) Antibody staining of MTs at stages of the cell cycle that correspond to Fig. 1A. In unbudded cells long MTs run through the cell (a). At the onset of budding two 'paired tubulin structures' (PTS, arrow in b) appear at the growth region, and are in contact with most MTs. During early bud growth the PTS remain close to the bud neck (arrow in c) and, based on the staining intensity, appear to nucleate bundles of MTs into the growing bud, whereas presumably single MTs extend into the mother cell (c). Prior to mitosis the PTS are positioned one behind the other (arrow in d) and originate arrays of long MTs into mother and daughter cell. At the onset of mitosis cytoplasmic MTs disappear and short spindles are formed (e). During mitosis two asters of microtubules emanate from the nuclei (arrowheads in f) and nuclei migrate to the center of mother and daughter cell, respectively. Finally, cytoplasmic MTs reappear (g), and the cell undergoes cytokinesis. Bars, 3 μm. (C) MTs in dikaryotic hyphae. MTs were decorated with anti-α-tubulin antibodies. Hyphae contain 2-5 long bundles of MTs (a), which often end in the middle of the tip cell (b). Most MTs have no contact with the hyphal tip (arrow in c) or with the septum (arrow in d). Bars, 3 μm (a); 2 μm (b-d).

and motility velocities were determined using Image-Pro Plus (Media Cybernetics). Sliding and MT translocation were typically a rapid and discontinuous motility event. Therefore, measurements of shrinking and growth of MTs in bundles excluded these motions and only continuous length changes spanning more than 3 frames (1 second) were taken into account. In budded cells almost all shortening was observed at ends distant from the neck region. Catastrophe values were defined as the number of transitions from growth to shrinkage per total time of growth, and rescue values reflect the number of transitions from shrinkage to growth per total time of shrinkage (according to Drummond and Cross, 2000, and references therein). To exclude the possibility that motion of single MTs might be a result of rapid polymerization at one end and depolymerization at the other (treadmilling), speckle microscopy experiments were done (Waterman-Storer et al., 1998). For these experiments we made use of the conditional mutant strain FB2rGFPTub1, in which the *crg*-promoter (Bottin et al., 1996) was fused to *GFPtub1* by homologous recombination. This construct allowed high expression of *GFPtub1* in complete medium containing 1% arabinose (CM-A) and repression of *GFPtub1* in CM supplemented with 1% glucose (CM-G), resulting in a controlled depletion of the GFP-Tub1 fusion protein. 6-8 hours after the shift to CM-G, labeling of MTs was drastically reduced and unlabelled patches appeared within MTs. These patches were used as landmarks on the MTs and allowed us to distinguish between length changes and motion of individual MTs.

Staining procedures

For indirect immunofluorescence of MTs, formaldehyde (EM-grade, Polyscience) was added to growing cultures to a final volume of 4% and cells were fixed for 30 minutes, washed with phosphate-buffered saline (PBS, pH 7.2) and applied to coverslips precoated with poly-L-lysine. This was followed by washes with PBS and 30 minutes of treatment with 3 mg/ml Novozyme (NovoNordisk). Subsequently cells were washed and incubated in 1% Triton X-100 for 1 minute, followed by additional washes and incubation in blocking reagent (2% milk powder, 2% BSA in PBS, pH 7.2) for 10 minutes. Antibodies against α-tubulin (N356, Amersham) and Cy3-, and Cy2-conjugated secondary antibodies (Dianova/Jackson Laboratories), were diluted in 0.2% milk, 0.2% BSA. 0.01% azide in PBS, pH 7.2 and applied for 60 minutes. For colocalization studies of GFP-MTs with tubulin antibodies, cells were fixed with 1-2% formaldehyde for 30 minutes and prepared for immunofluorescence as described above, except that 0.2% Triton X-100 was applied for 15 seconds.

Cytological studies of living cells were performed on logarithmically growing liquid cultures. For microscopic observation 5 μl cells were mixed with 5 μl 1% low melting agarose that was prewarmed at 36°C. Nuclear staining was done using cells fixed with 1% formaldehyde for 15 minutes followed by incubation with 1 μg/ml DAPI (Sigma) in PBS for 15 minutes at 65°C and subsequent PBS washes.

Inhibitor studies

All inhibitors were purchased from Sigma, and stocks of 1 mM benomyl, nocodazole, thiabendazole, taxol and cytochalasin D in DMSO were prepared and stored at –20°C. For inhibitor studies these drugs were added to growing cultures to 10 μM final concentration and cells were incubated for 30 minutes at room temperature under gentle shaking; effects on MTs were observed at the microscope. In control experiments, corresponding amounts of DMSO were added to the cultures. For halo assays 10 ml CM-A plates were overlaid with 5 ml 0.8% agarose, precooled to 50°C and 100 μl cell suspension added. Filter papers saturated with inhibitors were put on top of the plates. After 15 hours at 28°C cells had formed a lawn within the agarose, but due to the toxic effect of the inhibitors a clear halo around the filters was observed. The diameters of the halos were analyzed statistically.

RESULTS

The microtubule cytoskeleton undergoes polarization during bud growth

We analyzed MT organization during the cell cycle of haploid *U. maydis* cells by using a monoclonal antibody against α-tubulin. In growing liquid cultures most cells were unbudded and contained a single nucleus that was positioned in the cell center (Fig. 1Aa). At this stage antibodies detected 2-7 long tubulin structures running through the length of the cell (mean=4.1±1.6, *n*=20 cells; Fig. 1Ba), which were most likely bundles of MTs, as confirmed by in vivo observations of GFP-tubulin fusion protein (see below). At the onset of polar budding (Fig. 1Ab, arrow) a pair of two spherical tubulin structures appeared at the growth region, which focussed the MTs towards the bud (Fig. 1Bb, arrow). These paired tubulin structures (PTS) appeared to result from a gradual concentration of tubulin during early budding (Fig. 2Aa-e). Each spherical unit of these structures had a defined diameter (0.48±0.04 μm, *n*=10) and distance from each other (0.61±0.09 μm, *n*=10), and were found in 40-70% of all growing cells. While the bud elongated (Fig. 1Ac) the PTS remained in the proximal part of the daughter cell close to the neck (arrow in Fig. 1Bc). At this stage they radiated long MTs into the mother cell and 2-3 brightly stained bundles of MTs into the medium sized bud (Figs 1Bc, 2Af), whereas no MTs were nucleated by the nuclear spindle pole body (SPB). Prior to mitosis the nucleus migrated into the bud (Fig. 1Ad), while the PTS were still located in the neck region, radiating two arrays of MTs into both mother and daughter cell, respectively (Figs 1Bd, 2Ah). Interestingly, during these stages the PTS varied in shape, ranging from almost spherical (Fig. 1Bd) to more elongated (Fig. 2Ag,Bc-f), and often consisted of globular domains from which MTs were extruded out into the mother and daughter cell (Fig. 2Ba-f). At the onset of mitosis the DNA condensed within the bud (Fig. 1Ae). Cytoplasmic MTs and the tubulin structures disappeared and short spindles of approximately 1 μm were formed (Fig. 1Be), which elongated up to 4 μm before two condensed nuclei could be detected using DAPI staining. Only occasionally, short astral MTs were

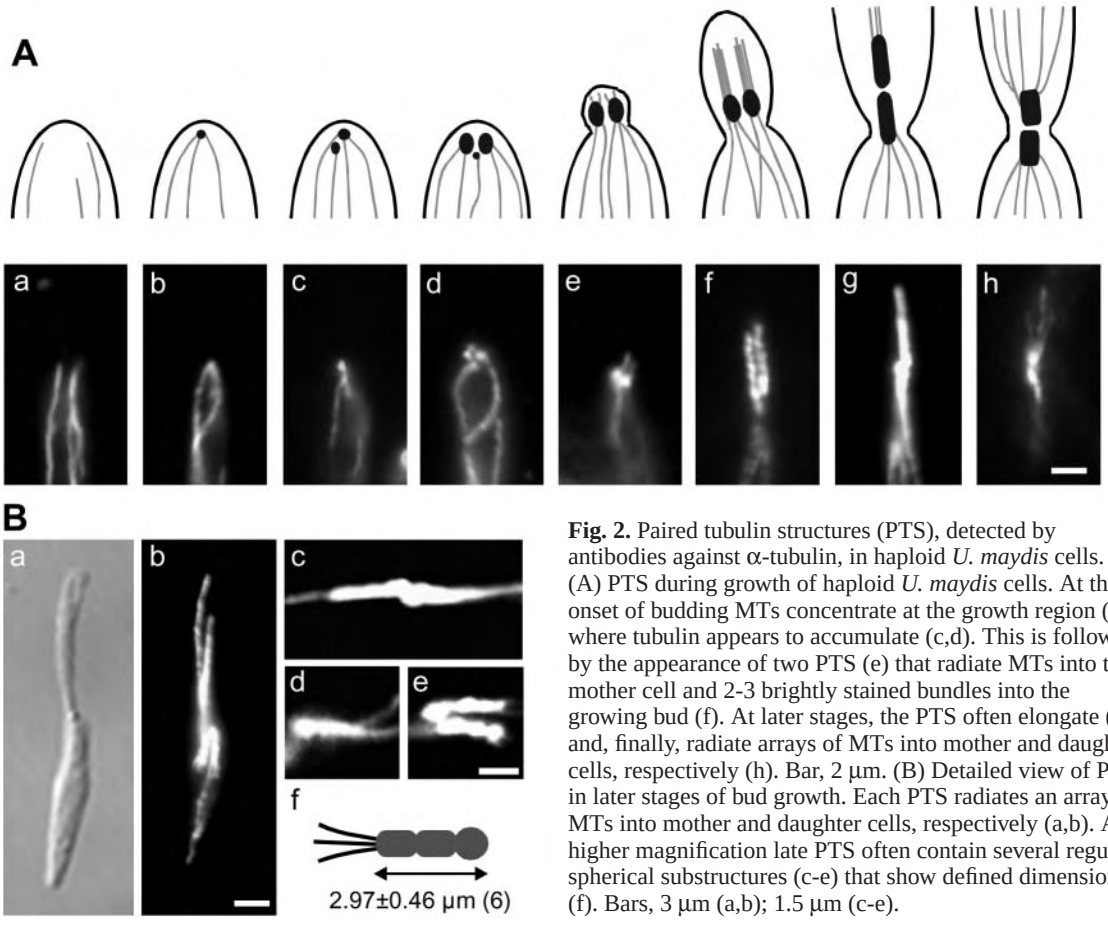

Fig. 2. Paired tubulin structures (PTS), detected by antibodies against α-tubulin, in haploid *U. maydis* cells. (A) PTS during growth of haploid *U. maydis* cells. At the onset of budding MTs concentrate at the growth region (a,b), where tubulin appears to accumulate (c,d). This is followed by the appearance of two PTS (e) that radiate MTs into the mother cell and 2-3 brightly stained bundles into the growing bud (f). At later stages, the PTS often elongate (g) and, finally, radiate arrays of MTs into mother and daughter cells, respectively (h). Bar, 2 μm. (B) Detailed view of PTS in later stages of bud growth. Each PTS radiates an array of MTs into mother and daughter cells, respectively (a,b). At higher magnification late PTS often contain several regular spherical substructures (c-e) that show defined dimensions (f). Bars, 3 μm (a,b); 1.5 μm (c-e).

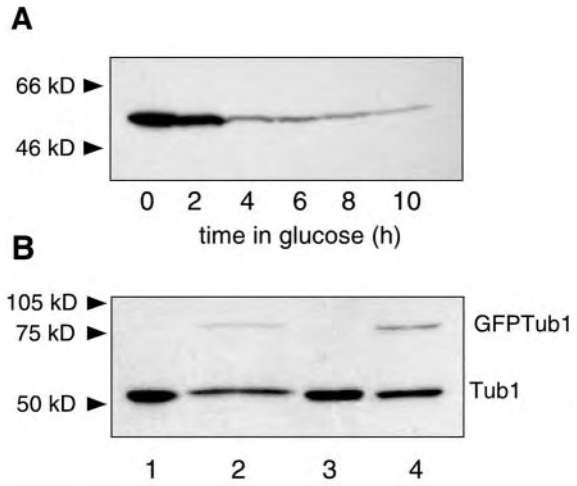

Fig. 3. Western blot analysis of conditional mutants in *tub1* and *GFP-tub1* expressing strains. (A) Western blot of cell extracts from a conditional *tub1* mutant (FB2rTub1) after shifting to restrictive conditions. Equal amounts of protein were loaded and separated by SDS-PAGE. The anti-α-tubulin antibody N356 (Amersham) was used to detect Tub1. After 4-10 hours the amount of cellular tubulin was drastically reduced; however, tubulin was not completely depleted. (B) Western blot of cell extracts from wild-type FB1 (lane 1), SG200 (lane 3) and *GFP-tub1* expressing strains FB1rGFPTub1 (lane 2) and SG200GFPTub1 (lane 4).

preserved during this stage (not shown). In contrast, asters of MTs were observed in late mitosis that appeared to emanate from the SPBs (Fig. 1Bf, arrowheads), while nuclear DNA was still condensed (Fig. 1Af). Finally, nuclei were positioned in the center of both cells (Fig. 1Ag) and SPB-independent MT bundles reappeared in mother and daughter cell, respectively (Fig. 1Bg).

Dikaryotic hyphae contained 2-5 bundles of MTs (Fig. 1Ca), which often ended in the middle of the hyphal tip cell (Fig. 1Cb). MTs usually had no contact with the apex (arrow in Fig. 1Cc) or with the septum of the growing tip cell (arrow in Fig. 1Cd).

Microtubules determine the polarity of the cell

The concentration of MT ends at one cell pole prior to bud formation suggested a role of the tubulin cytoskeleton in bud initiation and growth. To gain further insight into the cellular role of MTs we isolated an α-tubulin gene, *tub1*, by PCR using primers that were specific for α-tubulin (see Materials and Methods). The predicted amino acid sequence of Tub1 spans 448 amino acids and shares highest sequence similarity with α-tubulin from *Schizophyllum commune* (82% identity, not shown). We did not find indications for additional α-tubulin genes, either by PCR or low stringency Southern analysis (not shown). Therefore, it appeared that *tub1* was the only α-tubulin gene in *U. maydis* and its deletion was expected to be lethal. Consequently, we generated a conditional mutant strain, FB2rTub1, in which the *crg*-promoter (Bottin et al., 1996) was fused to *tub1* by homologous recombination (see Materials and Methods). This construct allowed expression of *tub1* in complete medium containing 1% arabinose (CM-A) and repression of *tub1* in CM supplemented with 1% glucose (CM-

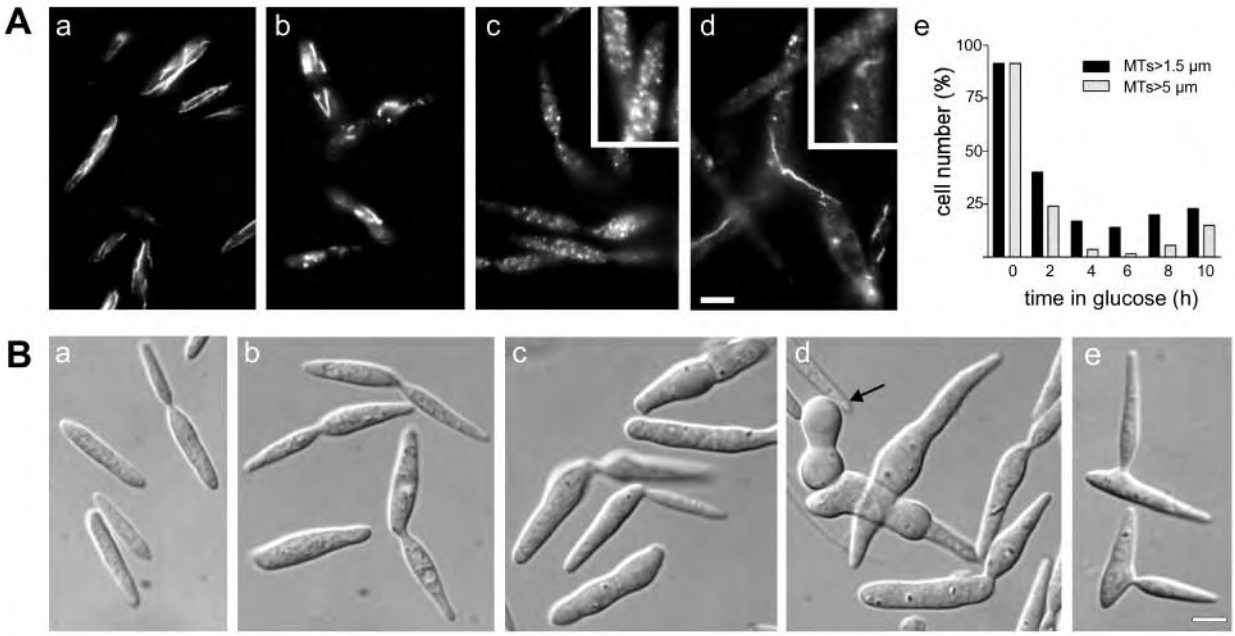

Fig. 4. Morphology in the absence of MTs. (A) MTs in FB2rTub1 grown under permissive (CM-A) and restrictive (CM-G) conditions. In CM-A almost all cells contain long MT bundles (a,e). After 2 hours growth in CM-G many cells contain only short or fragmented MTs (b,e), which almost completely disappear after 4 hours (e) and 6 hours (c,e). Surprisingly, the number and length of MTs per cell slightly increase after 10 hours growth in CM-G, while the punctuate cytoplasmic background almost disappears (detail in d, compare to detail in c). Note that the MT number did not further increase with longer growth in glucose containing medium (not shown). Graph is based on ≥100 cells per time point. Bar, 5 μm. (B) Morphological changes in FB2rTub1 mutants during growth under restrictive conditions. In CM-A cells showed normal morphology (a), but became thicker 5 hours (b) and 8 hours (c) after the shift to CM-G. After 10 hours many cells lost their polarity and rounded up (arrow in d), or showed lateral budding, suggesting a defect in determination of the polar growth site (e). Bar, 5 μm.

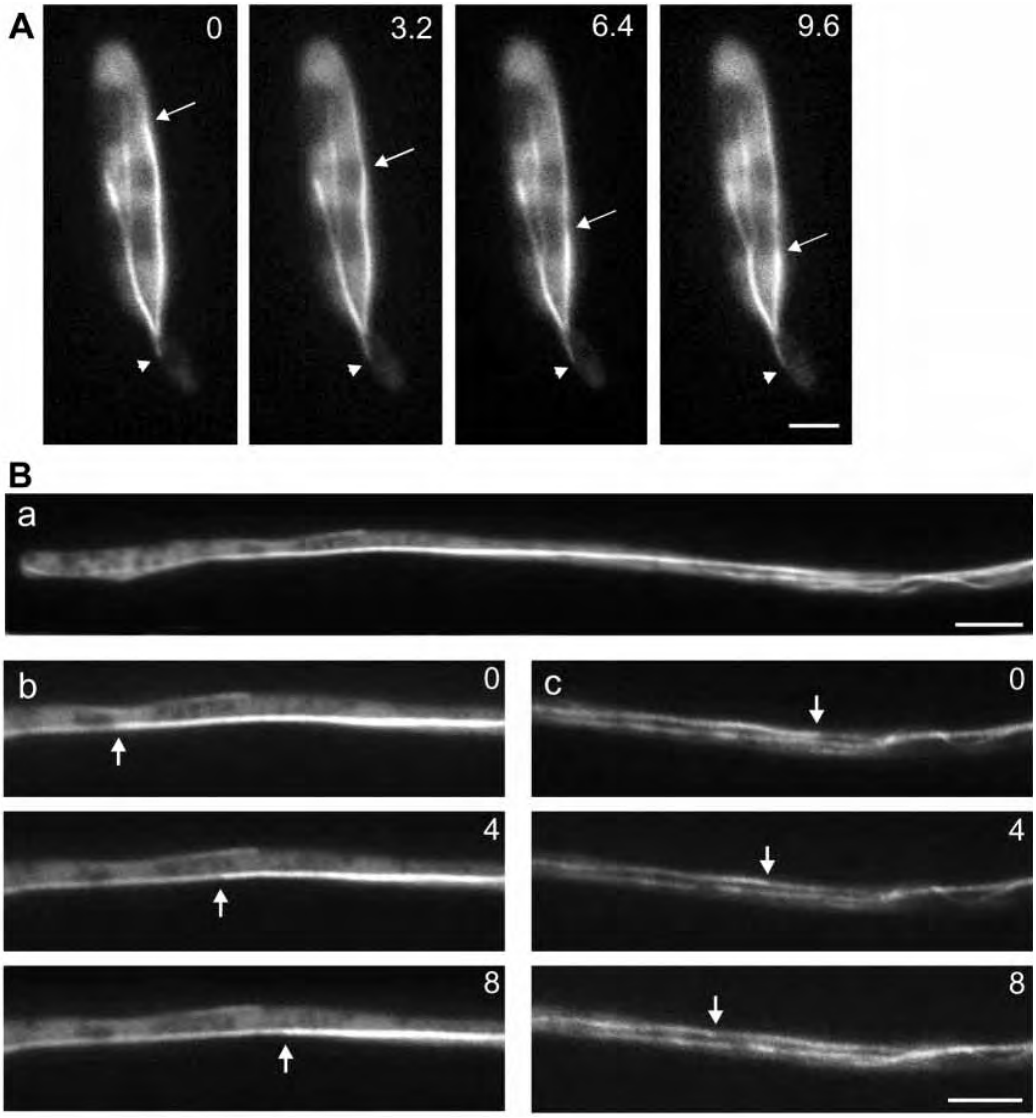

Fig. 5. Dynamics of MTs containing a GFP-Tub1 fusion protein in *U. maydis*. (A) A small budded cell of strain FB2rGFPTub1 with bundles of MTs that contain GFP-Tub1 fusion protein. Within these bundles single MTs show rapid depolymerization towards the neck region (arrow) and slow polymerization into the growing bud (arrowhead). Note that PTS were not visible in these cells. Bar, 3 μm. Time in seconds is given in the upper right corner. (B) GFP-Tub1 fusion protein in hyphae of *U. maydis*. A hypha of SG200rGFPTub1 contains long bundles of GFP-MTs (a), in which MT rapidly shorten towards the basal region (b, shrinking end of a microtuble marked by an arrow), while rapid shrinking towards the tip occurs in the subapical region of the same bundle (c, shrinking end of a microtuble marked by an arrow). Bars, 5 μm (a); 5 μm (b,c). Time in seconds is given in the upper right corner.

G). Western blot analysis revealed that shifting FB2rTub1 from CM-A to CM-G resulted in a drastic decrease of Tub1 within the first 4 hours (Fig. 3A), which lead to fragmentation of MTs after 2 hours (Fig. 4Ab) and a drastic decrease in MT number within 4-6 hours (Fig. 4Ac, Ae), while MT organization was normal in CM-A (Fig. 4Aa).

Interestingly, the anti-tubulin antibody detected a punctuate cytoplasmic staining of α-tubulin after 4-6 hours in CM-G (Fig. 4Ac, detail) that disappeared at 10 hours in CM-G (Fig. 4Ad, detail). This coincided with the reappearance of single MTs (Fig. 4Ad,e), whose number remained constant during extended growth in CM-G (not shown). The disappearance of MTs was accompanied by morphological changes of cells. In CM-A cells showed normal morphology (Fig. 4Ba), but became thicker after the shift to CM-G (Fig. 4Bb, 5 hours after shift; Fig. 4Bc, 8 hours after shift) until almost spherical cells were observed (arrow in Fig. 4Bd, 10 hours in CM-G). In addition, after 10 hours in CM-G FB2rTub1 cells showed lateral budding (Fig. 4Be), while this was not observed in the wild-type control. Such a role of MTs in bud formation was also confirmed by benomyl treatment, which disrupts MTs within 30 minutes (not shown). After 3 hours of drug treatment 43% of all cells (n=107) formed two or more buds that appeared mainly at the neck region. In addition, many buds grew at the opposing poles or at the lateral region of the cell (not shown). Such growth defects were not observed in the wild-type control cells treated with 0.5% DMSO, suggesting that, in the absence of MTs, both polar growth and growth site selection were impaired.

Expression of *GFP-tub1* has no effect on cell growth and microtubule organization

We fused GFP to the amino terminus of *tub1* and integrated this fusion construct into the succinate-dehydrogenase locus (Keon et al., 1991) of wild-type strains FB1, FB2 and the solopathogenic strain SG200, which grows filamentous on charcoal-containing plates and occasionally in liquid culture. Expression of the fusion construct either under the control of the *crg*-promoter (strains FB2rGFPTub1; SG200rGFPTub1) or the constitutive *otef*-promoter (strain FB1otefGFPTub1; for details see Materials and Methods) led to an incorporation of GFP-Tub1 fusion protein into MTs. The ratio of

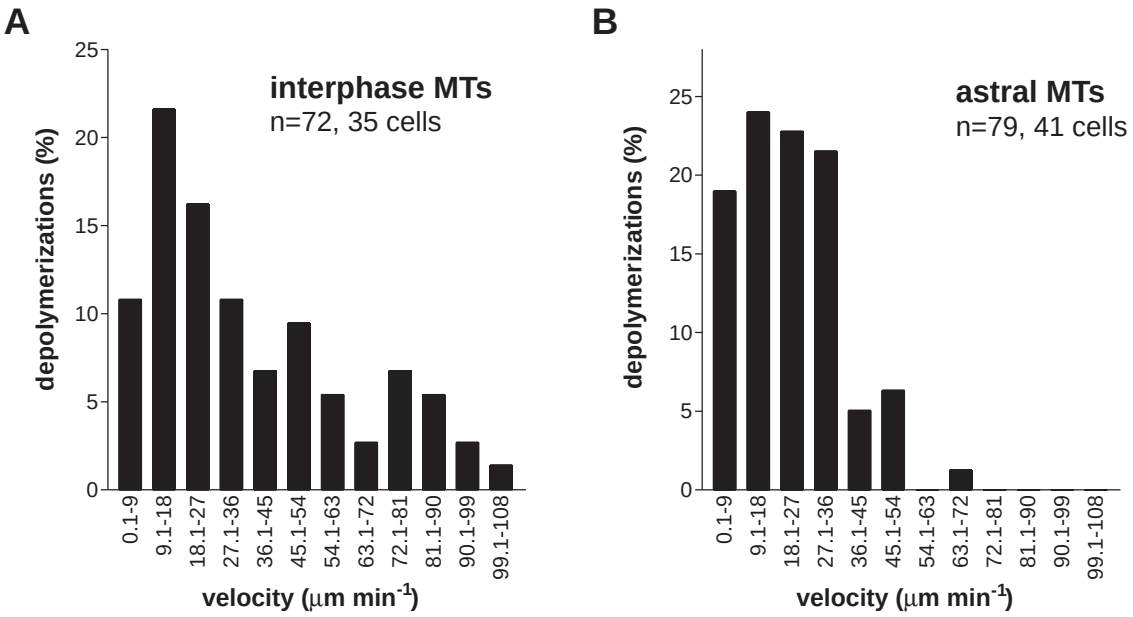

Fig. 6. MT depolymerization rates in FB2rGFPTub1. (A) SPB-independent MTs in interphase. In interphase MTs were usually bundled and showed rapid shrinking rates of up to 100 μm/minute. Note that short unbundled interphase MTs were not included. (B) SPB-nucleated MTs in mitosis. Note that no rapid shrinking occurs.

Tub1/GFP-Tub1 fusion protein in the cell was 3.4-6 for FB2rGFPTub1 and SG200rGFPTub1 (Fig. 3B) and approximately 1.5-2 for FB1otefGFPTub1 (not shown). The different levels of GFP-Tub1 fusion protein had no significant effect on depolymerization rates (not shown). Gentle fixation and treatment with low Triton X-100 concentrations preserved the GFP-signal and allowed double staining of GFP-MTs with tubulin antibodies. GFP-Tub1 fusion protein colocalized with the anti-tubulin antibody suggesting that it copolymerized with endogenous tubulin (not shown). Unfortunately, GFP-Tub1 was not incorporated into the paired tubulin structures and the two bundles that passed into the medium sized bud (Fig. 5A, compare Fig. 2Af). Moreover, the fusion protein could not complement for the depletion of Tub1 in FB2rTub1 under restrictive conditions, suggesting that the fusion protein is not fully active. Therefore, we thoroughly analyzed the growth and shape of *GFP-tub1* expressing strains at a statistical level. In addition, we compared the organization of MTs in FB1 as seen by antibody staining with the MT organization visualized by GFP-Tub1 fusion protein. Finally, we analyzed whether incorporation of GFP-Tub1 has any influence on MT stability by applying MT inhibitors that are known to modify MT dynamics. These experiments revealed that the expression of *GFP-tub1* affected neither cell shape nor doubling time of FB2rGFPTub1 or SG200rGFPTub1 compared to wild-type strains (P=0.2624 and 0.4023), and similarly for the number of MTs in FB2 and FB2rGFPTub1 (P=0.317). Moreover, in halo assays, treatment with benomyl, nocadazole, thiabendazole or taxol revealed no difference in sensitivity between wild-type control strains and *GFP-tub1* expressing strains to any of these drugs (not shown). In summary, these experiments demonstrate that, although not incorporated into the polar tubulin structures, expression of GFP-Tub1 did not negatively affect the cell, and, therefore, could be used to study in vivo dynamics of MTs.

Free and astral microtubules show dynamic instability

In vivo observation of GFP-Tub1 fusion protein in strain FB2rGFPTub1 and FB1otefGFPTub1, respectively, revealed four classes of microtubules: (1) long SPB-independent interphase MTs that were usually part of MT bundles, (2) short SPB-independent interphase MTs of 1-5 μm, which had no contact with other MTs and often showed rapid translocations within the cell, (3) SPB-bound and unbundled MTs that radiated into the cytoplasm during mitosis (astral MTs), and (4) spindle MTs. Interphase cells and hyphae contained 2-5 long filamentous structures that contained GFP-Tub1 (Fig. 5A,B). Shrinkage of these structures resulted either in their disappearance or in less intense staining (end of MTs marked by arrows in Fig. 5A,B), suggesting that these filaments either are single MTs or MT bundles. The rate of elongation of interphase MTs was approximately 10 μm/minute, which was not significantly different from that of astral MTs during mitosis in *U. maydis* (Tables 1, 2; P=0.6553). In addition, the frequency of switching from growth to shrinkage (catastrophe rate) was comparable for both MT types and similar to other values reported for fungi and vertebrate systems elsewhere (Tables 1, 2). On the other hand, shrinkage rates of long interphase MTs were significantly higher than those of astral MTs (P>0.0001). This was due to rapid shortenings at rates of 60-100 μm/minute (Fig. 6), which accounted for 15-18% of all depolymerization events in interphase and occurred almost exclusively within bundles (100% in FB1otefGFPTub1, n=80 in 45 cells; 91.7% in FB2rGFPTub1, n=72 in 35 cells). Interestingly, the difference did not depend on the cell cycle stage, as shrinkage rates of short unbundled interphase MTs and astral MTs in mitosis did not significantly differ (P=0.1833; Tables 1, 2). This suggests that there is a causal relationship between rapid depolymerization and MT bundling. Interestingly, switching from depolymerization to growth

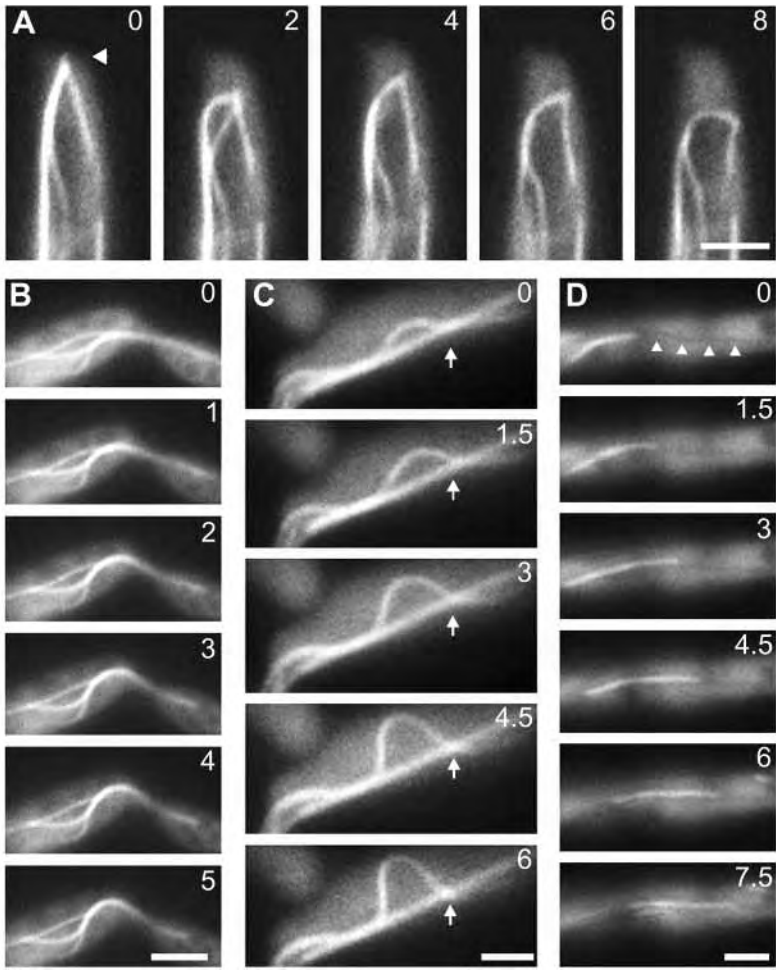

Fig. 7. Motility of MTs in *GFP-tub1* expressing strains in interphase. (A) Bending of MTs in FB1otefGFPTub1. MTs are focussed towards one cell pole (arrowhead). Cortical sliding of MTs appears to cause bending of the left bundle, demonstrating that MTs interact at the focus point. Note that bending is followed by a release and another bending. Bar, 3 μm. Time in seconds is given in the upper right corner. (B) Bending of a MT bundle in FB2rGFPTub1. No indications for MT interaction with the cortex are obvious, suggesting that bending results from sliding within the bundle. Bar, 3 μm. Time in seconds is given in the upper right corner. (C) Sliding and bending of a MT in FB2rGFPTub1. A stationary contact between MTs (arrows) appears to support this motion. Bar, 2 μm. Time in seconds is given in upper right corner. (D) Motion of a short MT along a filamentous track (arrows) that appears dark as it excludes the cytoplasmic background of GFP-Tub1 fusion protein in FB1otefGFPTub1. Note that the MT has no contact with other MTs. Bar, 3 μm. Time in seconds is given in the upper right corner.

(rescue) was almost never observed for interphase MTs, resulting in a remarkably low rescue rate (Table 1.)

In hyphae rapid depolymerization in opposite directions occurred at comparable frequency and velocity (Fig. 5B,C). Moreover, MTs grew towards both tip and septum of the hyphal cell. Neither polymerization rates nor rapid shrinking velocities differed with direction (elongation rate not different; P=0.1953; shrinking rate not different; P=0.5781). In addition, growth and shrinkage rates are not significantly different from that of haploid sporidia (P=0.1076 and 0.6998, respectively). Assuming that rapid depolymerization occurred at the 'plus-end' of the MTs towards their 'minus-ends' these data suggest that MTs have an anti-polar orientation within the MT bundles in hyphae. A similar situation was observed in unbudded *U. maydis* sporidia. In contrast, more than 90% of rapid shortenings were directed towards the neck region of budding cells (arrow in Fig. 5A), while MTs elongated towards the rear cell pole and into the bud (arrowhead in Fig. 5A). In budded cells MT ends that were close to the neck and presumably attached to the PTS did not show detectable activity. This indicates that during bud growth MT 'minus ends' are oriented towards the bud neck and that the PTS might support their formation and stabilization. However, this MT reorganization did not influence MT growth and shrinkage rates, as mean values did not differ between unbudded and budded cells in strains FB1otefGFPTub1 and FB2otefGFPTub1 (growth rate in unbudded cells: 11.14±4.14, n=39 MTs; growth rate in budded cells: 10.50±2.87, n=13; data sets not different, P=0.7998; shrinkage rate in unbudded cells: 40.08±19.92, n=171 MTs; shrinkage rates in budded cells: 40.89±19.84, n=65 MTs; data sets not different, P=0.6433).

Besides the described changes in length, single MTs and MT bundles frequently underwent bending and thereby often changed their location within the cell. Usually, entire bundles were bent (Fig. 7A,B). Occasionally, the polar focus point of

Table 1. Dynamics of non-centrosomal/SPB-independent microtubules

	Growth rate (μm/minute)	Shrinkage rate (μm/minute)	Catastrophe rate (transitions/second)	Rescue rate (transitions/second)
Squid axon[1]	1.14±0.42	7.98±1.08	n.d.	n.d.
A498[2]	6.9±2.5	8.4±5.5	0.031	0.114
Xenopus neuron[3]	10.6±1.91	9.7±2.28	0.012	n.d.
Ptk1[4]	11.0±3.7	14.8±7.5	n.d.	n.d.
Schizosaccaromyces pombe[5]	3.00±1.64	4.47±2.93	0.01667	0.031
Ustilago maydis[6] (long MTs)	10.77±2.41 (14)	37.76±17.7 (72)	0.04027 (10)	0.00736 (42)
Ustilago maydis[7] (short MTs)	3.95±2.30 (7)	20.12±15.65 (25)	n.d.	n.d.

All growth and shrinkage rates are given as means ± s.d. For definitions of catastrophe and rescue rates, see Materials and Methods.
[1]Seitz-Tutter et al., 1988; [2]Yvon and Wadsworth, 1997; [3]Tanaka and Kirschner, 1991; [4]Vorobjev et al., 1997; [5]Drummond and Cross, 2000.
[6]Long and mainly bundled MTs of FB2rGFPTub1 cells in interphase; number of MTs in parentheses.
[7]Short (<5 μm) and unbundled MTs of FB2rGFPTub1 cells in interphase; catastrophe and rescue rates were combined; note that all shrinking-data follow a non-Gaussian distribution; number of MTs in parentheses.

MTs was displaced (arrowhead in Fig. 7A), suggesting that MTs were not only oriented towards the cell pole but were held together by unknown structural components. In addition, presumably single MTs were bent by sliding across other MTs at a velocity of approximately 30 μm/minute (Fig. 7C, Table 3). This sliding often involved a single contact point (arrows in Fig. 7C) and, therefore, might reflect some MT bound motor activity that applied force on the neighboring MT and, thereby, caused bending of the polymer. MTs that underwent bending or sliding were excluded from any measurements of MT elongation or shrinking (see above). Moreover, elongation rates of randomly taken long and unbundled MTs did not differ from those organized in bundles (P=0.6128), suggesting that sliding within bundles is not a significant source of error for our polymerization/depolymerization data given in Tables 1 and 2.

In addition to sliding and bending we observed a third type of MT motility. In 10-15% of all haploid cells investigated (80 cells in both FB2rGFPTub1 and FB1otefGFPTub1) motion of short and unbundled MTs occurred (Figs 7D, 8A). Motile MTs had no contact with other MTs and moved over several μm at rates of approximately 40 μm/minute (Table 3), with maximal velocities up to 100 μm/minute. They showed normal depolymerization rates; however, elongation only rarely occurred at much slower rates (Table 1). MT motion usually followed defined cellular tracks that were occasionally visible as a dark line against the cytoplasmic background of GFP-Tub1 fusion protein (Fig. 7D, arrowheads), suggesting that a filamentous cytoskeletal element might support MT motion. Occasionally, several types of MT motion occurred within a sequence of 30 seconds (Fig. 8A). While one end of a newly formed MT kept in contact with a long MT (Fig. 8A, asterisk) the other end elongated (Fig. 8A, arrowhead). During growth the small MT slid along another MT at approx. 48 μm/minute (Fig. 8A, frames 2-5). It than remained stationary and the free end flipped direction, while the MT still elongated. This was followed by the detachment of the small MT and motion along the cortex at a rate of approx. 77 μm/minute (frames 8-10). We consider this complex moving behaviour to be most likely due to an unknown motor activity that underlies the MT motion in *U. maydis*. However, to exclude the possibility that MT motion results from rapid polymerization at one end and rapid shrinkage at the other end of a MT, a process called

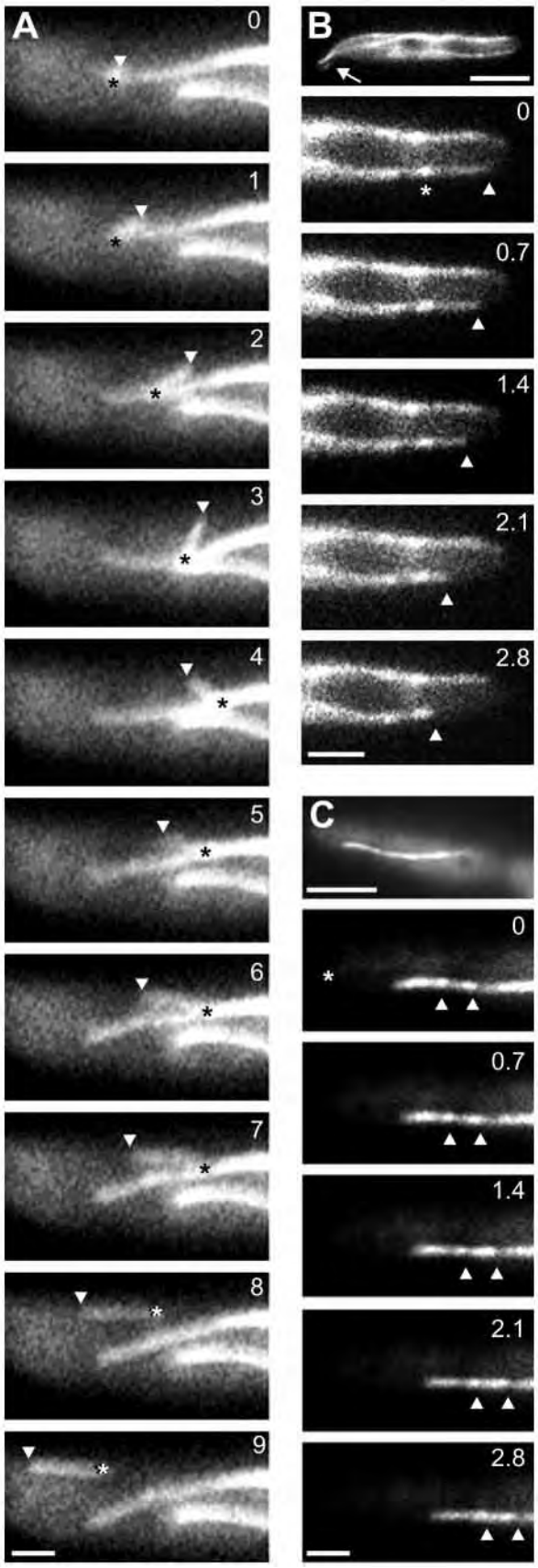

Fig. 8. Motion of free MTs and fluorescence speckle experiments. (A) Formation, sliding and cortical motion of a short free MT. A MT elongates while it remains attached to another MT (attached end marked by an asterisk). The attached end slides along this MT, while the other end (arrowhead) still elongates. As it gains contact with the cortex the short MT changes direction and subsequently detaches and rapidly moves along the cortex. Bar, 1 μm. Time in seconds is given in the upper right corner. (B) Depolymerization in a small budded cell of FB2rGFPTub1 after 6 hours under restrictive conditions. Under GFP-Tub1 depletion the fusion protein is unevenly incorporated in the MTs, resulting in dark areas and bright speckles (asterisk). The speckles remain stationary while depolymerization at a rate of 42 μm/minute towards the small bud occurs (bud marked by arrow in overview). Time in seconds is given in the upper right corner. Bars, 5 μm in overview and 2 μm in sequence. (C) Motion of a free MT in FB2rGFPTub1 after 6 hours under restrictive conditions. GFP-Tub1 is almost depleted and dark patches are formed along the length of the MT (arrowheads). These patches remain at a constant distance from the end while the MT is moving at a rates of approx. 11 μm/minute, suggesting that the complete MT is translocated. Time in seconds is given in the upper right corner. Bars, 5 μm in overview and 2 μm in sequence.

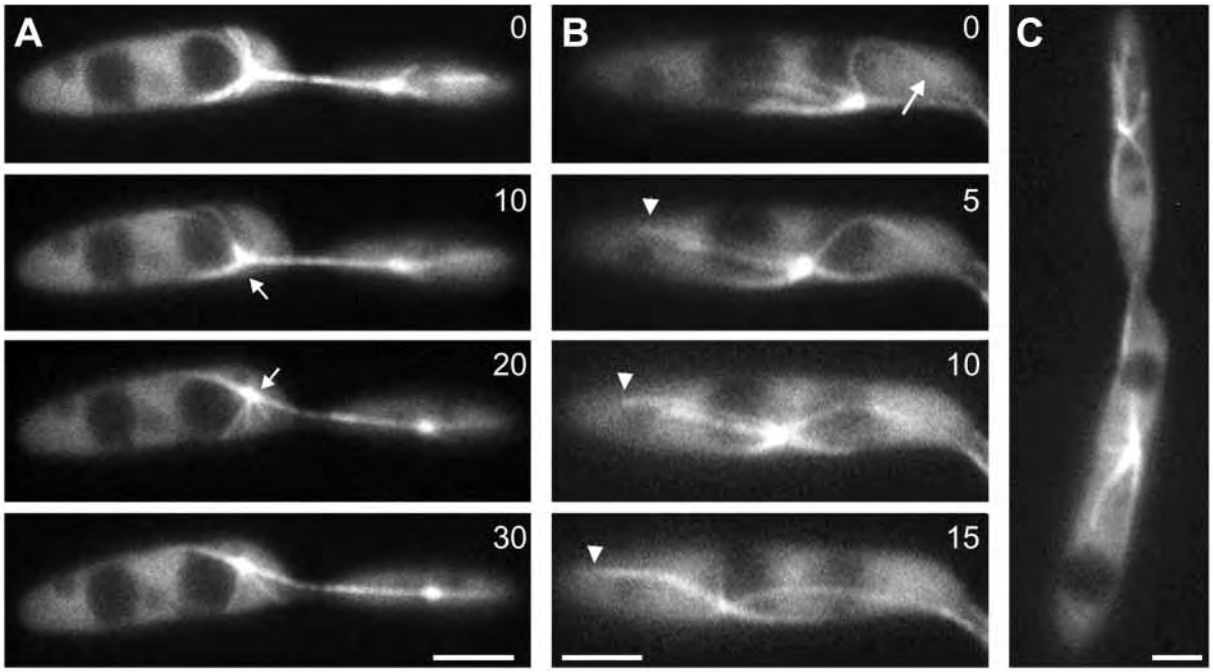

Fig. 9. Microtubules and nuclear migration. (A) In FB1oGFPTub1 a rigid bridge of spindle MTs connects two asters during anaphase B. Astral MTs have contact with the cortex and appear to exert a pulling force on the spindle poles, resulting in lateral motion of the aster (arrows). These forces most likely support spindle elongation during mitosis. Bar, 3 μm. Time in seconds given in the upper right corner. (B) Motion of a MT aster during late stages of mitosis within a mother cell (daughter cell to the right). Long astral MTs radiate into the cell and have contact with the cortex (arrowhead). This interaction appears to support movement of the aster and seems to pull the nucleus towards its final position within the cell center. Note that a flexible bridge between both nuclei still exists (arrow, bud neck to the right). Bar, 3 μm. Time in seconds is given in the upper right corner. (C) Prior to cytokinesis, nuclei are positioned within mother and daughter cell, respectively. Dynamic astral MTs kept contact with the cortex and prominent short range motion of the asters was observed. Bar, 3 μm.

treadmilling, we performed fluorescence speckle microscopy (Waterman-Storer et al., 1998). For this purpose we made use of very low expression levels of GFP-Tub1 protein in FB2rGFP-Tub1 grown for several hours under restrictive conditions (for details see Materials and Methods). Under these conditions, the cellular GFP-Tub1 level is drastically reduced, resulting in a very weak staining and an uneven incorporation of the remaining GFP-Tub1, leading to unlabelled patches within the MT (Fig. 8B,C). In case of treadmilling, these 'landmarks' on the MT should be stationary during length changes while the MT apparently moves. We observed this situation in MTs that rapidly depolymerized towards the neck region of small budded cells (Fig. 8B, bud in overview marked by an arrow). The bright speckle (asterisk) remained stationary while the MT depolymerized at a rate of approx. 42 μm/minute. In contrast, dark patches usually remained at a defined distance to the ends and moved with the motile MTs through the cell (Fig. 8C; asterisk marks the end of the cell), although these short MTs occasionally showed elongation and shrinkage (Table 1). This, again, strongly indicates that MT motion in *U. maydis* is an active transport process rather than a result of rapid length changes.

Nuclear migration is supported by microtubules

The nucleus remained positioned in the mother cell until it migrated into the bud prior to mitosis (Fig. 1A). At the onset of mitosis the SPB started to nucleate dynamic and short astral MTs. Occasionally, these MTs kept in contact with the cell cortex, suggesting that they might serve as an anchor for the spindle. After the mitotic spindle had elongated up to 2-3 μm

Table 2. Dynamics of centrosomal/astral microtubules

	Growth rate (μm/minute)	Shrinkage rate (μm/minute)	Catastrophe rate (transitions/second)	Rescue rate (transitions/second)
A498[1]	6.17±3.5	6.59±5.2	0.024	0.112
BSC-1[2]	7.6±3.6	15.0±12.5	0.043	0.071
Ptk1[3]	11.9±6.5	19.8±10.8	0.0606	0.1299
CHO1[3]	19.7±8.1	32.2±17.7	0.0541	0.1961
S. cerevisiae[4]	4.6±5.7	4.8±2.9	0.026	0.019
S. cerevisiae[5]	0.49±0.16	1.35±0.71	0.006	0.002
Ustilago maydis[6]	10.22±4.51 (19)	24.87±13.94 (79)	0.0324 (22)	0.0303 (23)

All growth and shrinkage rates are means ± s.d.

[1]Yvon and Wadsworth, 1997; [2]Dhamodharan and Wadsworth, 1995; [3]Shelden and Wadsworth, 1993; [4]Adames and Cooper, 2000, s.d. calculated from given s.e.m. and given sample size; [5]Carminati and Stearns, 1997, s.d. calculated from given s.e.m. and given sample size

[6]Based on observation of FB1otefGFPTub1 cells in telophase; number of MTs in parentheses.

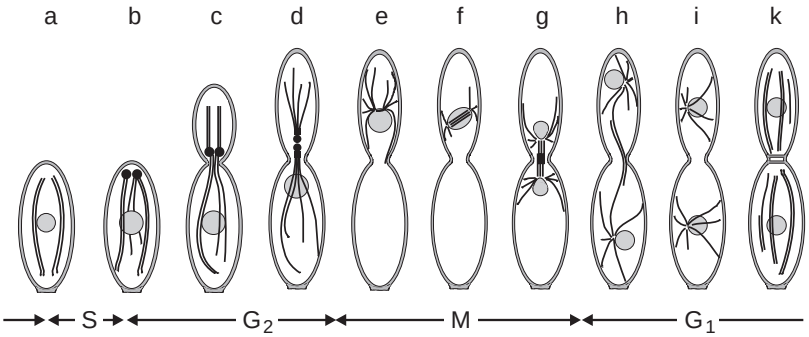

Fig. 10. MT organization and nuclear migration during the cell cycle of *U. maydis*. Cell cycle stages of *U. maydis* are taken from Snetselaar and McCann, 1997. During G_1 and second phase, unbudded cells contain bundles of anti-parallel MTs (a). At early G_1 the cytoskeleton become polarized and PTS appear at the growth region (b). While the bud enlarges these structures appear to nucleate MTs and radiate arrays into the mother cell and the growing bud, whereas the SPBs are inactive (c). Prior to mitosis, the nucleus migrates into the bud (d). After it reached the daughter cell the SPBs begin to nucleate spindle as well as astral MTs (e,f), which interact with the cortex and appear to anchor the nucleus during early mitosis. In anaphase the spindle migrates into the neck, where it rapidly elongates (g). This process appears to be supported by astral MTs that pull on the spindle poles. Prior to cytokinesis nuclei migrate towards the cell centers (h), and are supported by unknown motors that interact with astral MTs. Finally, both nuclei are positioned in the middle of mother and daughter cell, respectively (i), and bundles reappear (k). Note that the graph does not indicate the duration of each cell cycle stage.

it migrated towards the neck constriction at approx. 9 μm/minute (Table 3). This coincided with the appearance of long astral MTs, which radiated into the daughter and mother cell, respectively (Fig. 9A). The nucleus, stained with DAPI, elongated up to 4.67±0.84 μm (n=20) before the DNA separated (not shown). However, a rigid bridge of MTs, probably the anaphase B spindle, still connected the daughter nuclei (Fig. 9A), while astral MTs appeared to pull on the spindle thereby supporting lateral motion of the asters (arrows in Fig. 9A). At this stage the spindle continued to elongate slowly at a rate of approx. 4 μm/minute (Table 3). With increasing distance between the nuclei the MT bridge between them became thinner and more flexible (arrow in Fig. 9B). During this stage, the MT aster showed prominent to-and-fro motion, which gave way to sudden translocations over several μm at a mean velocity of approx. 21 μm/minute (Fig. 9B; Table 3). This motion appeared to be mediated by astral MTs that extended into the cytoplasm (Fig. 9B, arrowheads). Finally, the nuclei were repositioned in the cell center (Fig. 9C). At this stage, astral MTs still had contact with the cell cortex, resulting in short-range motion, again indicating that forces were exerted on the nuclei via astral MTs.

To confirm a role for MT in nuclear migration and positioning we shifted FB2rTub1 to restrictive conditions and subsequently analyzed the position of nuclei. Under permissive conditions 91% of the large budded FB2rTub1 cells (n=100) contained either condensed mitotic nuclei, which were located in the bud, or post-mitotic nuclei positioned in the mother and daughter cell, respectively, and there was no obvious difference from wild-type strains (not shown). In contrast, after 4 hours in CM-G, more than 65% of the large budded cells (n=102) contained condensed nuclei that were incorrectly positioned within the mother cell, suggesting that in the absence of MTs nuclear migration towards the bud was impaired, although DNA condensation occurred. In agreement, benomyl treatment for 45 minutes occasionally resulted in abnormal positioning of post-mitotic nuclei, and after 3 hours after incubation this treatment drastically inhibited nuclear migration into the bud, with 97% of all large budded cells (n=100) containing condensed nuclei in the mother cell. In summary, these results indicate that nuclear migration in G_2 is supported by SPB-independent MTs, while astral MTs mediate nuclear motility during mitosis.

Table 3. Motility rates of tubulin structures in *U. maydis*

	Velocity (μm/minute)
Motion of single short MTs*	41.19±24.40 (19)
Sliding/looping of MTs*	31.80±11.56 (8)
Spindle translocation in early anaphase	9.26±5.78 (6)
Spindle elongation in late anaphase	4.41±3.10 (6)
Aster motion in telophase	21.56±5.56 (15)

Values are means ± s.d. (n), based on the observation inFB1otefGFPTub1 and FB2rGFPTub1.
*Cells in interphase.

DISCUSSION

MT-dependent membrane trafficking is essential for fungal growth (Heath, 1995) and is thought to participate in the morphological transition between yeast and hyphal growth of pathogenic fungi (Akashi et al., 1994; Yokoyama et al., 1990). Here we demonstrate that MTs are focussed towards the growing bud and support polar growth of haploid *U. maydis* cells. During mitosis and early G_1 (Fig. 10), astral MTs that emanated from the SPBs supported nuclear migration and positioning. Interestingly, in vivo observation of GFP-MTs demonstrated that haploid cells as well as hyphae contained bundles of dynamic MTs, which had an anti-polar orientation and showed bending and translocation.

The paired tubulin structures resemble microtubule organizing centers

Prior to bud formation, the cytoskeleton of unbudded cells underwent polarization. MTs started to focus towards one cell pole and tubulin accumulated there, finally leading to the appearance of a pair of spherical tubulin structures (PTS), which appeared to organize MTs towards the growth region (Fig. 10). Unfortunately, PTS were not visible in *GFP-tub1* expressing strains; however, GFP-Tub1-containing MTs depolymerized towards the neck region, suggesting that the minus-ends of MTs are concentrated at or near the PTS. Interestingly, early PTS colocalized with minus-end directed cytoplasmic dynein (G. Steinberg, unpublished), supporting the conclusion that PTS mark the minus-ends of MTs. Consequently, the PTS might represent a SPB-independent microtubule-organizing centre (MTOC) that nucleates MTs during those stages of the cell cycle in which spindle poles are

not active. In *S. pombe*, spindle poles are also inactive during interphase (Masuda et al., 1992), and two cytoplasmic MTOCs, so-called post-anaphase arrays (PAA), appear at the end of anaphase, where they nucleate MTs that support nuclear migration (Hagan and Hyams, 1988). Therefore, the PAA and the PTS described here might be functional analogous structures, although electron microscopy revealed that PAA in *S. pombe* are ring-like and might release MTs to give rise to MT asters (reviewed in Hagan, 1998). Further ultrastructural studies will be needed to understand the detailed organization of PTS in *U. maydis*.

Interestingly, growth of yeast-like cells of *C. albicans* might also be supported by polar MTOCs. Immunostaining of *C. albicans* indicated that SPBs are inactive in unbudded cells and SPB-independent MTs are present in the unbudded cell (Barton and Gull, 1988). Similar to *U. maydis*, these MTs are focussed towards the growth region at the onset of bud formation. However, as no polar MTOCs are described for *C. albicans* it remains to be seen whether polar MT organizers are a common feature of the budding form of dimorphic fungi.

Microtubules support cell polarity

The polar organization of MTs and defects in polar budding and growth of *tub1*-mutant strains argue for an involvement of MTs in vectorial transport towards the growth region, which is in agreement with recent findings that MT-dependent trafficking of endosomes is required for polar growth of *U. maydis* (Wedlich-Söldner et al., 2000). Such a function of MTs corresponds to recent reports on MT function in polar growth of *S. pombe*. Disruption of MTs with thiabendazole (Sawin and Nurse, 1998), as well as defects in the MT cytoskeleton in mutant strains, led to abnormal growth and the establishment of lateral growth sites (reviewed in Hagan, 1998; Mata and Nurse, 1998) that was probably due to impaired MT-dependent transport of polarity determining components, like Tea1 (Mata and Nurse, 1997) or F-actin (Sawin and Nurse, 1998), towards the cell poles. In agreement, disruption of MTs led to lateral budding in *U. maydis*, suggesting that MTs serve similar functions in fission yeast and *U. maydis*. However, the organization of MTs by polar MTOCs during bud growth of *U. maydis* is fundamentally different from *S. pombe*.

Surprisingly, although repression of *tub1* in FB1rTub1 led to rapid fragmentation of MTs, the antibody still recognized α-tubulin dots in the cytoplasm. These dots disappeared after 8-10 hours under restrictive conditions, which coincided with the reappearance of some MTs. At present we consider it most likely that repression of *tub1* disturbed some equilibrium of tubulin and associated factors, which led to rapid MT disruption when α-tubulin was repressed; later, the system recovered, thereby recruiting the residual Tub1 to newly formed MTs.

GFP-Tub1 is incorporated into microtubules but not PTS

GFP-Tub1 fusion protein was incorporated into MTs and did not influence cell shape, growth and MT stability. This is in agreement with previous studies showing that GFP-α tubulin was fully biologically active and its expression had no detectable effect on *S. cerevisiae* (Carminati and Stearns, 1997) and *S. pombe* (Ding et al., 1998). However, *U. maydis* GFP-tubulin fusion could not complement for the deletion of endogenous α-tubulin and, in addition, did not incorporate itself into PTS of *U. maydis*. We find it likely that steric hindrance account for the latter defect. Therefore, cells that only produce GFP-Tub1 fusion protein might not be able to form these structures. As discussed above, PTS have a key role in organizing the MT cytoskeleton during budding. Therefore, we find it most likely that an inability to form PTS accounts for the restricted activity of GFP-Tub1 fusion protein, while incorporation into MTs has no detectable effect on the cell.

Microtubule dynamics of *U. maydis* are similar to vertebrate cells

Growth and shrinkage rates of MTs are reported for a wide spectrum of cell types. In vertebrate cells growth rates are 8-20 μm/minute, while shrinkage occurs at higher velocity with mean rates of 10-32 μm/minute (see Tables 1 and 2). In contrast, recent studies on *S. cerevisiae* (Carminati and Stearns, 1997; Adames and Cooper, 2000) and *S. pombe* (Drummond and Cross, 2000) indicated that fungal MTs might exhibit significantly slower elongation and shortening velocities. In *U. maydis* interphase and astral MTs showed polymerization at mean rates of approx. 10 μm/minute and rapid depolymerization at mean rates of approx. 38 and 25 μm/minute, respectively. These values are most similar to Ptk1 and CHO1 cells (Shelden and Wadsworth, 1993; see Tables 1, 2) and clearly demonstrate that neither slow growth nor reduced shrinkage rates are a feature of all fungal MTs. On the other hand, interphase MTs of *U. maydis* showed unusual rapid depolymerization events with rates up to 100 μm/minute that were restricted to MTs within bundles. Moreover, once depolymerization has taken place, switching to polymerization, a process reflected by the rescue rate, almost never occurred (Table 1). These results indicate that the mechanisms and control of MT depolymerization of bundled interphase MTs are specific for *U. maydis* and might differ from other fungal and vertebrate cell systems. On the other hand, we cannot completely rule out the possibility that sliding between MTs within a bundle might add to rapid depolymerizations. However, elongation rates of randomly taken bundled and long unbundled MTs did not differ, indicating that sliding within bundles is not significantly falsifying our growth and shrinkage data.

Interphase cells and hyphae contain bundles of anti-polar microtubules

Rapid depolymerization and slower polymerization of MTs occurs most often at the plus-end of MTs while the minus-ends are often stabilized by components of the MTOC (see Maddox et al., 2000; Wiese and Zheng, 2000). MT-dependent motor proteins utilize the polarity of MTs with most kinesins moving towards the ‘plus ends’, whereas dynein-mediated transport is ‘minus end’ directed. Therefore, knowledge of MT polarity is important for understanding intracellular transport processes in fungal hyphae (see Morris et al., 1995).

Our in vivo observations indicate that hyphae and unbudded haploid cells contain SPB-independent MT filaments. Rapid shortening within these structures leave less intensively stained MTs behind. Therefore, we consider it most likely that these filaments are MT bundles and it would be interesting to see whether ultrastructural data support this conclusion. Within these bundles rapid depolymerization occurs in both directions, indicating that MTs have an antipolar orientation. This

conclusion is supported by former studies on MTs in hyphae of *U. maydis* (Steinberg et al., 1998). In this study, anti-tubulin antibodies and MT inhibitors were used to show that recovery of MTs starts at both the apex and the basal region of the hyphal tip cell and it was speculated that SPB-independent hyphal MTs are organized in an antiparallel fashion (Steinberg et al., 1998). Such a mixed polarity of MTs was described for dendrites (Baas et al., 1988) raising the possibility that neurons and fungal hyphae are similar with respect to MT-dependent long-distance transport.

Similar motors might support microtubule motility and mitotic nuclear migration

In *U. maydis* mitosis occurs within the bud and chromosome segregation coincides with rapid nuclear migration. Our *in vivo* observations show that the SPB does not nucleate MTs during pre-mitotic nuclear motion, although nuclear migration into the bud is a MT-dependent process. Ultrastructural studies on *U. maydis* demonstrated that the SPB localizes to the leading edge of the migrating nucleus (O'Donell and McLaughlin, 1984), suggesting that the SPB might slide along stationary MTs, a mechanism also discussed for *S. pombe* (Hagan, 1998). In contrast, later stages of nuclear migration in *U. maydis* are supported by astral MTs emanating from the SPB that have contact with the cortex. Forces applied to these MTs appear to pull on the nuclei, thereby supporting anaphase B and nuclear migration during mitosis. Such a mechanism is well established for fungi (see Hagan and Hyams, 1996; Inoue et al., 1998; Adames and Cooper, 2000), and it is most likely that cortical dynein is involved in this process (reviewed in Steinberg, 2000).

Interestingly, MTs showed rapid movement and bending during interphase of haploid *U. maydis* cells. Such motility was not described for fungal cells; also bending of single GFP-MTs occurs upon contact with the cell poles in *S. pombe*, a process which most likely results from compression of the elongating MT (Drummond and Cross, 2000). However, bending of interphase MTs is a common feature of animal cells (Cassimeris et al., 1988; Seitz-Tutter et al., 1988; Tanaka and Kirschner, 1991). Remarkably, MT translocation in axons appears to be a MT independent mechanism, suggesting that cortical actin could be involved (Ahmad and Baas, 1995), which appears to anchor cytoplasmic dynein and thereby supports MT transport in neurons (Ahmad et al., 1998). Moreover, cortical MT sliding supports nuclear migration in *S. cerevisiae* and dynein is assumed to participate in this process (Carminati and Stearns, 1997; Adames and Cooper, 2000). In *U. maydis*, MTs move along unknown filamentous tracks, suggesting that similar transport mechanisms involving F-actin and dynein might account for this process. This raises the intriguing possibility that dynein participates in motion, sliding and looping of MTs in *U. maydis*; however, the molecular details of MT motility remain to be elucidated.

What is the cellular function of MT motility in *U. maydis* cells? It was argued that MT translocation supports axon elongation and neuronal growth (Tanaka and Kirschner, 1991) and helps to organize the MT cytoskeleton in epithelial cells (Mogensen, 1999). In contrast to polar axons, however, translocation of MT in *U. maydis* was often observed in unbudded cells that are not growing. It is important to note that most MT translocations were found in cells that contained a disrupted MT cytoskeleton. Therefore, short motile MTs might be MT fragments, rather than being a defined class of MTs, a notion that is supported by the rare and unusual slow polymerization of these short MTs (Table 1). Consequently, cortical translocation of short MTs might be without biological relevance, but reflects a cytoplasmic motor activity that participates organization of MT bundles in interphase and rearrangement during polar growth.

Conclusion

In contrast to *S. cerevisiae*, where MTs almost exclusively function in nuclear migration and chromosome segregation (Madden and Snyder, 1998), MTs play a key role in morphogenesis and cell polarity of *U. maydis*. Such a role of MTs is reminiscent of *S. pombe*, and similarities in MT organization with that of *C. albicans* suggest that our results for *U. maydis* reflect the significance of MTs for fungal morphogenesis and cellular organization in general. The dynamic parameters provided in this study demonstrate that MT dynamics in fungal cells could be within the range of vertebrate systems. Moreover, the existence of MT bending and cortical MT sliding in *U. maydis* will provide a new means for investigating the molecular basis and cellular role of these types of intracellular motility.

We are grateful to Drs R. Kahmann and M. Feldbrügge for stimulating discussions and helpful suggestions on the manuscript. We wish to thank M. Artmeier for technical help. This work was supported by the Deutsche Forschungsgemeinschaft (SFB 413). The *tub1* nucleotide sequence reported in this paper has been submitted to the GenBank/EMBL Data Bank with the accession number Hx975089759.

REFERENCES

Adames, N. R. and Cooper, J. A. (2000). Microtubule interactions with the cell cortex causing nuclear movements in *Saccharomyces cerevisiae*. *J. Cell Biol.* **149**, 863-874.

Agrios, G. N. (1999). *Plant Pathology*. San Diego, London, Boston, New York, Sydney, Tokyo, Toronto: Academic Press.

Ahmad, F. J. and Baas, P. W. (1995). Microtubules released from the neuronal centrosome are transported into the axon. *J. Cell Sci.* **108**, 2761-2769.

Ahmad, F. J., Echeverri, C. J., Vallee, R. B. and Baas P. W. (1998). Cytoplasmic dynein and dynactin are required for the transport of microtubules into the axon. *J. Cell Biol.* **140**, 391-401.

Akashi, T., Kanbe, T. and Tanaka, K. (1994). The role of the cytoskeleton in the polarized growth of the germ tube in *Candida albicans*. *Microbiol.* **140**, 271-280.

Baas, P. W., Deitch, J. S., Black, M. M. and Banker, G. A. (1988). Polarity orientation of microtubules in hippocampal neurons: uniformity in the axon and nonuniformity in the dendrite. *Proc. Natl. Acad. Sci. USA* **85**, 8335-8339.

Banuett, F. (1995). Genetics of *Ustilago maydis*, a fungal pathogen that induces tumors in maize. *Annu. Rev. Genet*. **29**, 179-208.

Banuett, F. and Herskowitz, I. (1989). Different a alleles of *Ustilago maydis* are necessary for maintenance of filamentous growth but not for meiosis. *Proc. Natl. Acad. Sci. USA* **86**, 5878-5882.

Barton, R. and Gull, K. (1988). Variation in cytoplasmic microtubule organization and spindle length between the two forms of the dimorphic fungus *Candida albicans*. *J. Cell Sci.* **91**, 211-220.

Bibikova, T. N., Blancaflor, E. B. and Gilroy, S. (1999). Microtubules regulate tip growth and orientation in root hairs of *Arabidopsis thaliana*. *Plant J.* **17**, 657-665.

Bölker, M., Genin, S., Lehmler, C. and Kahmann, R. (1995a). Genetic regulation of mating and dimorphism in *Ustilago maydis*. *Can. J. Bot.* **73**, 320-325.

Bölker, M., Bohnert, H. U., Braun, K. H. and Kahmann, R. (1995b). Tagging pathogenicity genes in *Ustilago maydis* by restriction enzyme-mediated integration (REMI). *Mol. Gen. Genet.* **248**, 547-552.

Bottin, A., Kämper, J. and Kahmann, R. (1996). Isolation of a carbon source-regulated gene from *Ustilago maydis*. *Mol. Gen. Genet.* **253**, 342-352.

Bradford, M. M. (1976). A rapid and sensitive method for the quantitation of microgram quantities of protein utilizing the principle of protein-dye binding. *Anal. Biochem.* **72**, 248-253.

Carlile, M. J. (1995). The success of the hypha and mycelium. In *The Growing Fungus* (ed. N. A. R. Gow and G. M. Gadd), pp. 3-19. London: Chapman & Hall.

Carminati, J. L. and Stearns, T. (1997). Microtubules orient the mitotic spindle in yeast through dynein-dependent interactions with the cell cortex. *J. Cell Biol.* **138**, 629-641.

Cassimeris, L., Pryer, N. K. and Salmon, E. D. (1988). Real-time observations of microtubule dynamic instability in living cells. *J. Cell Biol.* **107**, 2223-2231.

Desai, A. and Mitchison, T. J. (1997). Microtubule polymerization dynamics. *Annu. Rev. Cell Dev. Biol.* **13**, 83-117.

Dhamodharan, R. and Wadsworth, P. (1995). Modulation of microtubule dynamic instability in vivo by brain microtubule associated proteins. *J. Cell Sci.* **108**, 1679-1689.

Ding, D.-Q., Chikashige, Y., Haraguchi, T. and Hiraoka, Y. (1998). Oscillatory nuclear movement in fission yeast meiotic prophase is driven by astral microtubules, as revealed by continuous observation of chromosomes and microtubules in living cells. *J. Cell Sci.* **111**, 701-712.

Drummond, D. R. and Cross, R. A. (2000). Dynamics of interphase microtubules in *Schizosaccharomyces pombe*. *Curr. Biol.* **10**, 766-775.

Gow, N. A. R. (1995). Yeast-hyphal dimorphism. In *The Growing Fungus* (ed. N. A. R. Gow and G. M. Gadd), pp. 403-422. London: Chapman & Hall.

Hagan, I. M. (1998). The fission yeast microtubule cytoskeleton. *J. Cell Sci.* **111**, 1603-1612.

Hagan, I. M. and Hyams, J. S. (1988). The use of cell division cycle mutants to investigate the control of microtubule distribution in the fission yeast *Schizosaccharomyces pombe*. *J. Cell Sci.* **89**, 343-358.

Hagan, I. M. and Hyams, J. S. (1996). Forces acting on the fission yeast anaphase spindle. *Cell Motil. Cytoskel.* **34**, 69-75.

Heath, I. B. (1995). The cytoskeleton. In *The Growing Fungus* (ed. N. A. R. Gow and G. M. Gadd), pp. 99-134. London: Chapman & Hall.

Holliday, R. (1974). *Ustilago maydis*. In *Handbook of Genetics* (ed. R. C. King), New York: Plenum Press.

Inoue, S., Yoder, O. C., Turgeon, B. G. and Aist, J. R. (1998). A cytoplasmic dynein required for mitotic aster formation in vivo. *J. Cell Sci.* **111**, 2607-2614.

Jacobs, C. W., Mattichak, S. J. and Knowles, J. F. (1994). Budding patterns during the cell cycle of the maize smut pathogen *Ustilago maydis*. *Can. J. Bot.* **72**, 1675-1680.

Joshi, H. C. (1998). Microtubule dynamics in living cells. *Curr. Opin. Cell Biol.* **10**, 35-44.

Keon, J. P., White, G. A. and Hargreaves, J. A. (1991). Isolation, characterization and sequence of a gene conferring resistance to the systemic fungicide carboxin from the maize smut pathogen, *Ustilago maydis*. *Curr. Genet.* **19**, 475-481.

Lehmler, C., Steinberg, G., Snetselaar, K. M., Schliwa, M., Kahmann, R. and Boelker, M. (1997). Identification of a motor protein required for filamentous growth in *Ustilago maydis*. *EMBO J.* **16**, 3464-3473.

Madden, K. and Snyder, M. (1998). Cell polarity and morphogenesis in budding yeast. *Ann. Rev. Microbiol.* **52**, 687-744.

Maddox, P., Chin, E., Mallavarapu, A., Yeh, E., Salmon, E. D. and Bloom, K. (1999). Microtubule dynamics from mating through the first zygotic division in the budding yeast *Saccharomyces cerevisiae*. *J. Cell Biol.* **144**, 977-987.

Maddox, P. S., Bloom, K. S. and Salmon, E. D. (2000). The polarity and dynamics of microtubule assembly in the budding yeast *Saccharomyces cerevisiae*. *Nature Cell Biol.* **2**, 36-41.

Mallavarapu, A., Sawin, K. and Mitchison, T. (1999). A switch in microtubule dynamics at the onset of anaphase B in the mitotic spindle of *Schizosaccharomyces pombe*. *Curr. Biol.* **9**, 1423-1426.

Masuda, H., Sevik, M. and Cande, W. Z. (1992). In vitro microtubule-nucleating activity of spindle pole bodies in fission yeast *Schizosaccharomyces pombe* cell cycle-dependent activation in *Xenopus* cell-free extracts. *J. Cell Biol.* **117**, 1055-1066.

Mata, J. and Nurse, P. (1997). Tea1 and the microtubular cytoskeleton are important for generating global spatial order within the fission yeast cell. *Cell* **89**, 939-949.

Mata, J. and Nurse, P. (1998). Discovering the poles in yeast. *Trends Cell Biol.* **8**, 163-167.

Mogensen, M. (1999). Microtubule release and capture in epithelial cells. *Biol. Cell.* **91**, 331-341.

Morris, N. R., Xiang, X. and Beckwith, S. M. (1995). Nuclear migration advances in fungi. *Trends Cell Biol.* **5**, 278-282.

Nabi, I. R. (1999). The polarization of the motile cell. *J. Cell Sci.* **112**, 1803-1811.

O'Donell, K. L. and McLaughlin, D. J. (1984). Postmeiotic mitosis, basidiospore development, and septation in *Ustilago maydis*. *Mycologia*. **76**, 486-502.

Sambrook, J., Fritsch, E. F. and Maniatis, T. (1989). *Molecular Cloning, A Laboratory Manual.* Cold Spring Harbour Laboratory Press.

Sawin, K. E. and Nurse, P. (1998). Regulation of cell polarity by microtubules in fission yeast. *J. Cell Biol.* **142**, 457-471.

Schulz, B., Banuett, F., Dahl, M., Schlesinger, R., Schaefer, W., Martin, T., Herskowitz, I. and Kahmann, R. (1990). The B alleles of *Ustilago maydis* whose combinations program pathogenic development code for polypeptides containing a homeodomain-related motif. *Cell* **60**, 295-306.

Seitz-Tutter, D., Langford, G. M. and Weiss, D. G. (1988). Dynamic instability of native MTs from squid axon is rare and independent of gliding and vesicle transport. *Exp. Cell Res.* **178**, 504-512.

Shaw, S. L., Yeh, E., Maddox, P., Salmon, E. D. and Bloom, K. (1997). Astral microtubule dynamics in yeast. A microtubule-based searching mechanism for spindle orientation and nuclear migration into the bud. *J. Cell Biol.* **139**, 985-994.

Shelden, E. and Wadsworth, P. (1993). Observation and quantification of individual microtubule behavior in vivo: microtubule dynamics are cell type specific. *J. Cell Biol.* **120**, 935-945.

Snetselaar, K. M. and McCann, M. P. (1997). Using microdensitometry to correlate cell morphology with the nuclear cycle in *Ustilago maydis*. *Mycologia* **89**, 689-697.

Spellig, T., Bottin, A. and Kahmann, R. (1996). Green fluorescent protein (GFP) as a new vital marker in the phytopathogenic fungus *Ustilago maydis*. *Mol. Gen. Genet.* **252**, 503-509.

Steinberg, G. (2000). The cellular role of molecular motors in fungi. *Trends Microbiol.* **4**, 162-168.

Steinberg, G. and Schliwa, M. (1995). The *Neurospora* organelle motor: a distant relative of conventional kinesin with unconventional properties. *Mol. Biol. Cell.* **6**, 1605-1618.

Steinberg, G., Schliwa, M., Lehmler, C., Bölker, M., Kahmann, R. and McIntosh, J. R. (1998). Kinesin from the plant pathogen *Ustilago maydis* is involved in vacuole formation and cytoplasmic migration. *J. Cell Sci.* **111**, 2235-2246.

Tanaka, E. and Kirschner, M. (1991). Microtubule behavior in the growth cone of living neurons during axon elongation. *J. Cell Biol.* **115**, 345-363.

Vorobjev, I. A., Svitkina, T. M. and Borisy, G. G. (1997). Cytoplasmic assembly of microtubules in cultured cells. *J. Cell Sci.* **110**, 2635-2645.

Waterman-Storer, C. M., Arshad, D., Bulinski, J. C. and Salmon, E. D. (1998). Fluorescent speckle microscopy, a method to visualize the dynamics of protein assemblies in living cells. *Curr. Biol.* **8**, 1227-1230.

Wedlich-Söldner, R., Bölker, M., Kahmann, R. and Steinberg, G. (2000). A putative endosomal t-SNARE links exo- and endocytosis in the phytopathogenic fungus *Ustilago maydis*. *EMBO J.* **19**, 1974-1986.

Wiese, C. and Zheng, Y. (2000). A new function for the γ-tubulin ring complex as a microtubule minus-end cap. *Nature Cell Biol.* **2**, 358-364.

Yamamoto, A., West, R., McIntosh, J. R. and Hiraoka, Y. (1999). A cytoplasmic dynein heavy chain is required for oscillatory nuclear movement of meiotic prophase and efficient meiotic recombination in fission yeast. *J. Cell Biol.* **145**, 1233-1249.

Yokoyama, K., Kaji, H., Nishimura, K. and Miyaji, M. (1990). The role of microfilaments and microtubules in apical growth and dimorphism of *Candida albicans*. *J. Gen. Microbiol.* **136**, 1067-1075.

Yvon, A. M. C. and Wadsworth, P. (1997). Non-centrosomal microtubule formation and measurement of minus end microtubule dynamics in A498 cells. *J. Cell Sci.* **110**, 2391-2401.